



# Enlarged capacitance of TiO<sub>2</sub> nanotube array electrodes treated by water soaking

Chi Zhang<sup>1</sup>, Ji Xing<sup>1</sup>, Haowen Fan<sup>1</sup>, Weikang Zhang<sup>1</sup>, Maoying Liao<sup>1</sup>, and Ye Song<sup>1,\*</sup>

<sup>1</sup>Key Laboratory of Soft Chemistry and Functional Materials of Education Ministry, Nanjing University of Science and Technology, Nanjing 210094, China

**Received:** 20 September 2016

**Accepted:** 14 November 2016

**Published online:**

17 November 2016

© Springer Science+Business Media New York 2016

## ABSTRACT

Anodic TiO<sub>2</sub> (ATO) nanotube arrays have been considered as promising electrode materials for super capacitors. However, their specific capacitance value is still not comparable with conventional super capacitor materials. Here, we demonstrate a convenient method for improving the capacitive properties of ATO nanotube arrays for super capacitors, which can be realized simply by soaking the as-anodized ATO nanotube arrays in water at room temperature for a sufficiently long time. The nanotube wall for the soaked ATO nanotube arrays becomes rough, resulting in increased specific surface area. After an electrochemical hydrogenation doping process using potentiodynamic cycling for the ATO samples, the soaked ATO electrodes exhibit a very high average specific capacitance of 20.96 mF cm<sup>-2</sup> at a current density of 0.05 mA cm<sup>-2</sup>, about a threefold improvement over those unsoaked ones that just treated by the electrochemical hydrogenation doping. The presented results demonstrate that the soaking treatment is a facile and cost-effective way to change the morphology of ATO nanotubes and increase specific capacitance, which would be of great industrial interest.

## Introduction

Anodic TiO<sub>2</sub> (ATO) nanotube arrays have attracted considerable attention because of their high surface area, unique electronic properties, excellent chemical stability, and environmental friendliness [1–7]. Recently, ATO nanotube arrays have gained growing interest as a promising electrode material for super capacitors [8–11], because the vertically oriented nanotube arrays provide a direct pathway for electron transport along the long axis of nanotubes to the

Ti foil substrate and can be employed directly as a super capacitor electrode. However, TiO<sub>2</sub> electrodes generally exhibit inferior capacitive behavior due to poor electrochemical activity and low electrical conductivity [12–17]. To promote their super capacitive performances, attempts have been made through a variety of materials engineering approaches including doping (hydrogen, niobium, and nickel) or modification of TiO<sub>2</sub> material, decorating the structure with an extra layer nanoparticles, and fabricating special geometry of TiO<sub>2</sub> nanotubes [18–23]. Recently,

Address correspondence to E-mail: soong\_ye@sohu.com

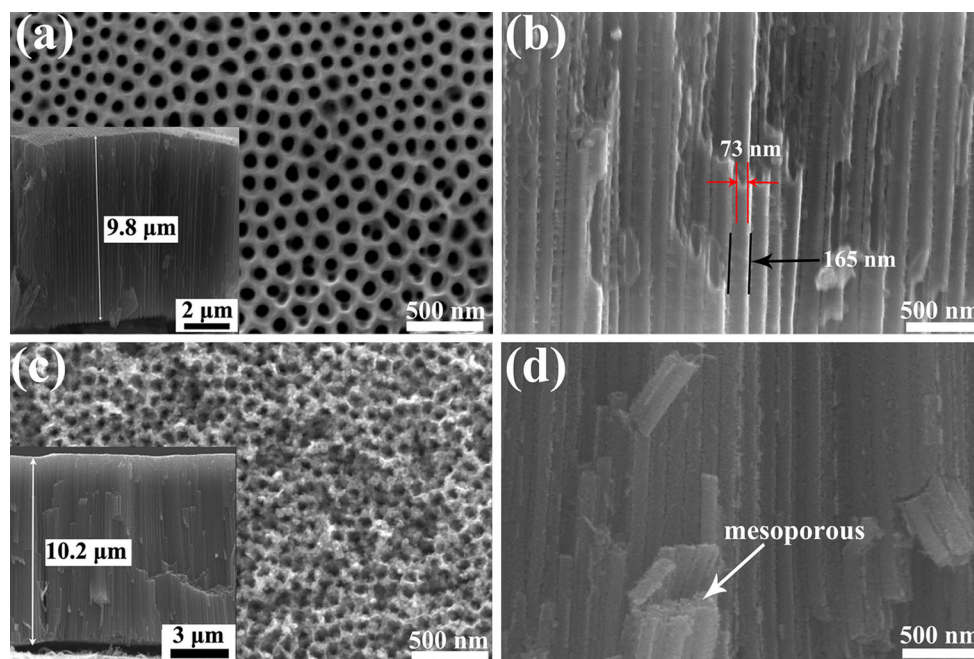


**Figure 1** FESEM images of **a** top view, **b** side view of the unsoaked ATO and **c** top view, **d** side view of the soaked ATO. The insets show the corresponding nanotube length of the

Lu et al. [8] have shown that hydrogenation, i.e., annealing in hydrogen atmosphere at high temperatures can improve significantly the electrochemical performance of ATO as super capacitor materials. They found that ATO nanotube arrays hydrogenated at 400 °C achieved the highest specific capacitances of  $3.24 \text{ mF cm}^{-2}$  with excellent rate capability and long-term stability. We have demonstrated that a plasma-assisted hydrogenation method can improve the electronic conductivity and electrochemical performances of ATO nanotube films [18]. The doped ATO nanotubes deliver a very high average specific capacitance of  $7.22 \text{ mF cm}^{-2}$  at a current density of  $0.05 \text{ mA cm}^{-2}$ . Zhou et al. [13] also showed that the electrochemically doped ATO nanotubes achieved a capacitance of  $0.949 \text{ mF cm}^{-2}$  at a current density of  $10 \text{ } \mu\text{A cm}^{-2}$ . Nevertheless, these specific capacitance values are still not comparable with conventional active materials such as  $\text{RuO}_2$  [24–26]. Hence, it is highly desirable to further increase their specific capacitance.

ATO nanotubes were found to store charge mainly via a double-layer capacitor fashion rather than a pseudo capacitive redox process [27, 28]. Increasing the effective surface area of ATO nanotubes should result in a higher areal specific capacitance [29].

unsoaked and soaked ATO nanotubes. Both ATO samples were treated by thermal annealing and the electrochemical hydrogenation doping.

Therefore, one of the most straightforward and effective methods for enhancing capacitance of ATO nanotubes is to increase their surface areas. Recently, a water treatment process to change geometry of  $\text{TiO}_2$  nanotubes has been reported [30, 31]. This motivated us to explore the effect of the water treatment process on the specific capacitance of ATO nanotubes. In this study, we present a facile approach to tune the morphology of nanotubes and improve their surface areas simply by soaking the as-anodized ATO nanotube arrays in water at room temperature for a sufficiently long time. It was demonstrated that the soaked ATO nanotube arrays showed a markedly improved capacitance compared with the unsoaked ones.

## Experimental

ATO nanotube array films were fabricated by two-step anodization of Ti foils in a two-electrode configuration. The first-step anodization was performed at 60 V for 2 h in an ethylene glycol electrolyte containing 0.5 wt%  $\text{NH}_4\text{F}$  and 2 vol%  $\text{H}_2\text{O}$ . The as-obtained nanotube films were removed from the Ti foil with adhesive tape. The second-step anodization was performed at 60 V for 1 h. The details were described

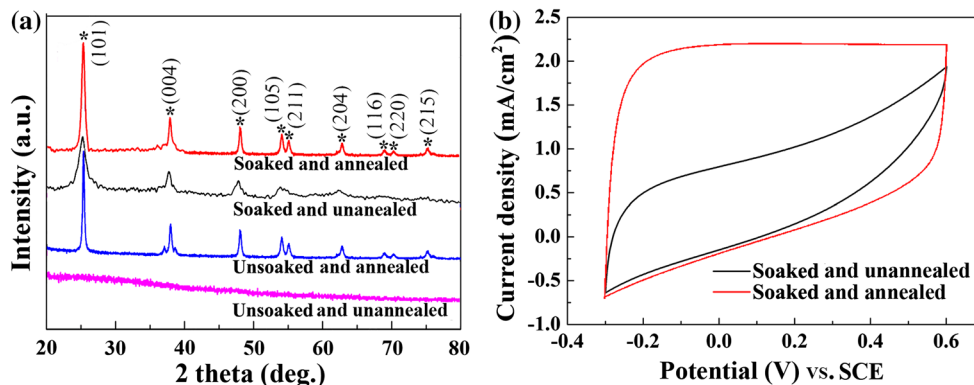


**Figure 2** **a** XRD patterns of ATO nanotube samples. **b** Cyclic voltammograms of the soaked ATO films obtained at a scan rate of  $100 \text{ mV s}^{-1}$  before and after thermal annealing.

elsewhere [18, 32, 33]. Afterward, the as-anodized ATO nanotube films were soaked in deionized water at room temperature for 80 h. The soaked ATO samples were annealed in air at  $150 \text{ }^\circ\text{C}$  for 2 h, then up to  $450 \text{ }^\circ\text{C}$  for 3 h to fully form  $\text{TiO}_2$  anatase phase. Finally, an electrochemical hydrogenation doping for ATO samples was performed in  $0.5 \text{ M Na}_2\text{SO}_4$  solution by potentiodynamic cycling between  $-2.2$  and  $0 \text{ V}$  at a scan rate of  $100 \text{ mV s}^{-1}$ . The ATO samples were characterized by field emission scanning electron microscopy (FESEM, NOVA Nano SEM 230) and X-ray diffraction (XRD) measurements (Bruker D8 Advance diffractometer with  $\text{Cu-K}\alpha$  radiation). All electrochemical measurements were carried out in  $2 \text{ M Li}_2\text{SO}_4$  aqueous solution in three-electrode compartments at room temperature using AUTOLAB PGSTAT302 N/FRA2. ATO samples (exposed area  $1 \times 1 \text{ cm}^2$ ), saturated calomel electrode (SCE), and Pt mesh served as the working, reference, and counter electrodes, respectively. Unless otherwise noted, all ATO samples were annealed in air and treated by the electrochemical hydrogenation doping before electrochemical tests. Cyclic voltammetry (CV) and galvanostatic charge–discharge tests were performed over a potential range from  $-0.3$  to  $0.6 \text{ V}$ . The cycling stability was tested using a continuous charge–discharge cycling at a current density of  $0.10 \text{ mA cm}^{-2}$ .

## Results and discussion

The FESEM micrographs of the unsoaked and soaked ATO nanotube arrays are shown in Fig. 1. For the unsoaked ATO nanotube arrays, it is shown from Fig. 1a that they possess a smooth top surface, with

an inner diameter of  $\sim 70 \text{ nm}$ , a wall thickness of  $\sim 40 \text{ nm}$ , and a tube length of about  $9.8 \text{ }\mu\text{m}$ . The unsoaked ATO nanotubes also have a smooth tube wall without any specific structure, as evident in Fig. 1b. After the soaking in water over 80 h, there exist so many small particles on the top surface of ATO nanotubes that they nearly block the nanopores of nanotube arrays, as shown in Fig. 1c. A length of about  $10.2 \text{ }\mu\text{m}$  of the soaked ATO nanotubes is quite similar to that of the unsoaked ones ( $9.8 \text{ }\mu\text{m}$ ), indicating that the soaking treatment does not change the length of ATO samples. Nevertheless, the tube wall becomes so thick and rough that hollow tubular-like structure is hard to observe (Fig. 1d); that is, nanotubes are converted into nanoparticulate aggregations. Obviously, the soaked ATO nanotubes with this microscopic morphology should have higher surface area than that of the unsoaked ones, which is consistent with literature reports [30, 31].

XRD patterns of the unsoaked and soaked ATO nanotube films are shown in Fig. 2a. For comparison, the XRD patterns of both ATO nanotubes before thermal annealing are also given in Fig. 2a. Clearly, the as-anodized (i.e., the unsoaked and unannealed) ATO nanotubes are in a fully amorphous state because of the absence of diffraction peaks. After thermal annealing, the unsoaked ATO films are transformed from amorphous to anatase phase. For the soaked ATO samples regardless of whether they were further annealed or not, the anatase  $\text{TiO}_2$  peaks can be clearly observed (JCPDS No. 21-1272). Therefore, in addition to thermal annealing, the as-anodized amorphous ATO films can also be transformed into crystalline anatase  $\text{TiO}_2$  by the soaking treatment. Besides, the phase transformation

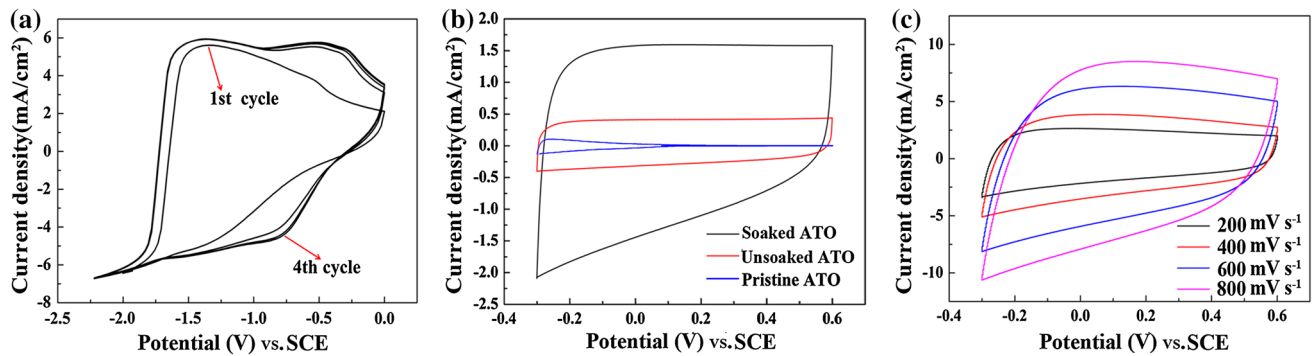


**Figure 3** a Consecutive cyclic voltammograms of the soaked ATO samples during potentiodynamic cycling process at a scan rate of  $100 \text{ mV s}^{-1}$ . b Cyclic voltammograms of the pristine,

unsoaked, and soaked ATO nanotubes. c Cyclic voltammograms of the soaked ATO nanotubes at different scan rates.

resulting from the soaking treatment leads to the morphology change of ATO films (Fig. 1). However, the crystallinity of the soaked samples is obviously enhanced after thermal annealing, which can be demonstrated by the increase of the peak intensities and the decrease of half-width in the anatase diffraction patterns (Fig. 2a). This means that the as-anodized ATO films can only be transformed into crystalline anatase  $\text{TiO}_2$  partially via water soaking. Moreover, the soaked samples that were not subjected to thermal annealing show a sloping cyclic voltammogram as shown in Fig. 2b, suggesting a poor performance of super capacitors with a higher electrode resistance [34]. In contrast, the soaked samples exhibit a nearly rectangular cyclic voltammogram with a greatly increased integrated area upon annealing. Therefore, prior to the electrochemical hydrogenation doping, all ATO samples were thermally annealed in this work.

As mentioned in “Introduction” section, the hydrogenation treatments can improve significantly the electrochemical performance of ATO as super capacitor materials due to an increased conductivity of  $\text{TiO}_2$  through self-doping [8, 18]. By contrast, the hydrogenation doping based on the electrochemical approach is more convenient and cost efficient for the treatment of ATO nanotube films. For instance, Zhou and Zhang [13, 35] reported a simple cathodic polarization method to achieve self-doped ATO nanotubes. They found that ATO nanotubes, polarized cathodically at  $-1.4 \text{ V}$  (vs. SCE) for the period of 10 min at room temperature, exhibited the highest capacitance of  $1.84 \text{ mF cm}^{-2}$  at a scan rate of  $5 \text{ mV s}^{-1}$  (39 times higher than that of the pristine  $\text{TiO}_2$ ). Here, we modified their electrochemical

hydrogenation method, i.e., the electrochemical doping process was performed by potentiodynamic cycling rather than by potentiostatic approach. Thus, the electrochemical hydrogenation process can be monitored by consecutive cyclic voltammograms of the samples. Once the recorded cyclic voltammograms tended to be stable and overlap, the electrochemical doping process would be finished. Figure 3a illustrates the typical cyclic voltammograms for the soaked ATO samples during the electrochemical doping process, where the cyclic voltammograms start to overlap after four potentiodynamic cycles. Usually, the electrochemical doping process for ATO samples can be completed within ten potentiodynamic cycles. Figure 3b presents cyclic voltammograms for the pristine (i.e., undoped), unsoaked ATO, and soaked ATO electrodes at a scan rate of  $100 \text{ mV s}^{-1}$ , respectively. It can be seen that the electroactivity of pristine ATO is very low at the anodic end of the cycles owing to its high resistance at high potentials [36], indicating its poor capacitive behavior. After the electrochemical doping, the unsoaked ATO electrode shows the excellent electroactivity over the whole potential range and a nearly rectangular cyclic voltammogram typical of double-layer capacitors [37, 38]. Clearly, the cyclic voltammogram of the unsoaked ATO electrode exhibits a larger integrated area and higher current response than that of the pristine ATO electrode, implying a markedly enhanced capacitive behavior after the electrochemical doping as reported previously [1, 13, 35]. The improved performances can be attributed to an increase in conductivity of  $\text{TiO}_2$  due to the introduced oxygen vacancies [13, 32].

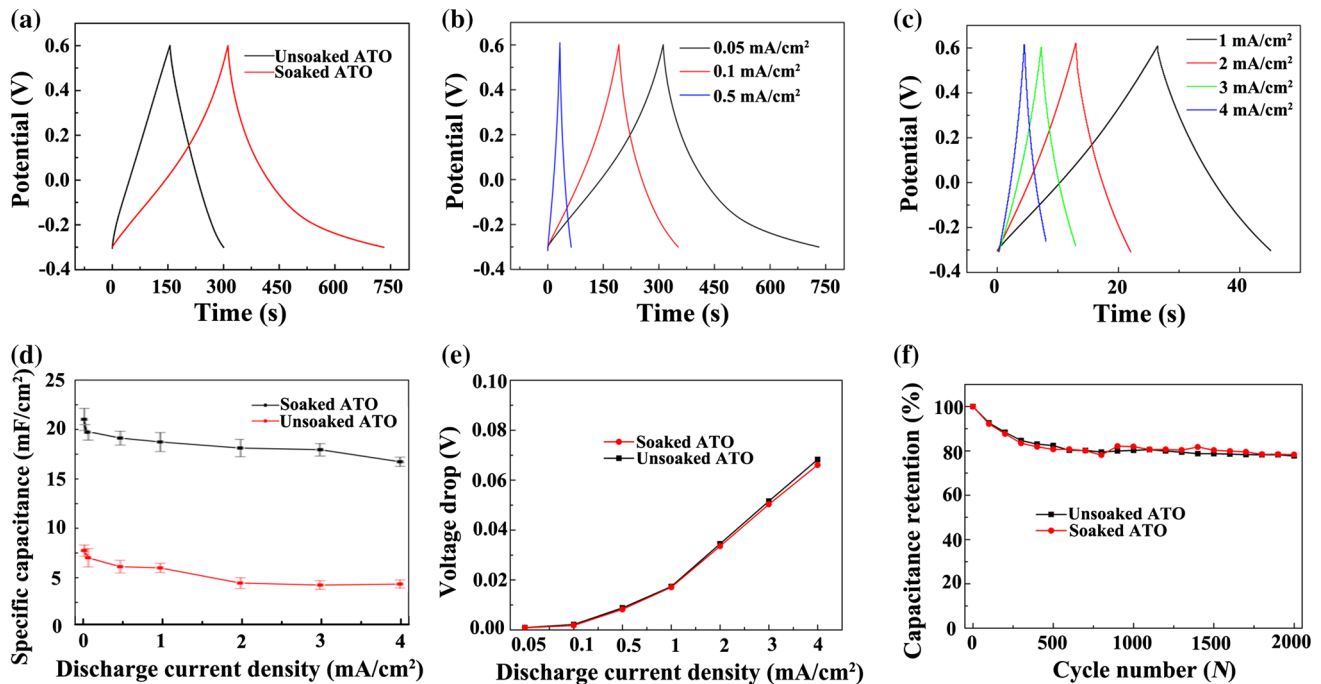


**Figure 4** **a** Comparison of galvanostatic charge–discharge plots of both ATO samples collected at a current density of  $0.05 \text{ mA cm}^{-2}$ . Galvanostatic charge–discharge curves of the soaked ATO nanotubes obtained from **b**  $0.05$  to  $0.50 \text{ mA cm}^{-2}$  and **c**  $1.00$  to  $4.00 \text{ mA cm}^{-2}$ . **d** The average areal capacitances for both ATO

nanotubes at different discharge current densities. **e** The voltage drops for both ATO nanotubes at different discharge current densities. **f** Capacitance retention versus cycle number for the soaked and the unsoaked ATO electrodes over 2000 cycles.

The soaked ATO nanotubes with nanoparticulate morphology, as described above, should have higher surface area, which in turn leads to a much higher capacitance. Wang et al. [30] reported that the soaked ATO nanotubes have a markedly improved surface area, about 5.5 times higher than that of the as-anodized ATO nanotubes. The cyclic voltammogram of the soaked ATO nanotubes in Fig. 3b confirms this conclusion. The cyclic voltammogram for the soaked ATO electrode has a considerably larger integrated area compared with the unsoaked one, revealing a dramatically enlarged capacitance after the soaking treatment. Figure 3c shows the cyclic voltammograms for the soaked ATO electrode at different scan rates over the wide range from  $0.2$  to  $0.8 \text{ V s}^{-1}$ . Significantly, the curves can still keep quasi-rectangular shape as the scan rate is up to  $0.8 \text{ V s}^{-1}$ , suggesting the excellent capacitive behavior and high rate capability of the soaked ATO electrode.

The super capacitive performances for the soaked ATO nanotubes are also evaluated by galvanostatic charge–discharge tests at different current densities. Figure 4a compares the charge–discharge curves of the unsoaked and soaked ATO nanotubes collected at

a current density of  $0.05 \text{ mA cm}^{-2}$ . Evidently, the charge–discharge curve of the soaked ATO electrode is substantially broadened compared to the unsoaked one, confirming an enhanced capacitance. As shown in Fig. 4b, c, the nearly symmetric and linear charge–discharge curves at different current densities indicate good coulombic efficiency of the soaked ATO electrodes. Figure 4d compares the average specific capacitances at various current densities for the unsoaked and soaked ATO electrodes. The soaked ATO electrode delivers a high average specific capacitance of  $20.96 \text{ mF cm}^{-2}$  at  $0.05 \text{ mA cm}^{-2}$ , almost three times larger than that of the unsoaked one. As expected, for both ATO electrodes, the specific capacitance decreases with increasing current density because of the limited ion diffusion. Nonetheless, both ATO electrodes show a slight decrease in capacitance, i.e., an outstanding rate capability. For example, the soaked electrode has a capacitance retention of  $80.1\%$  as the discharge current density increases from  $0.05$  to  $4.00 \text{ mA cm}^{-2}$ , though it has a higher specific capacitance than the unsoaked one. Besides, voltage drops for the both ATO electrodes are relatively small at all operated

current densities and very close to each other as shown in Fig. 4e. This indicates that both ATO electrodes have an excellent conductivity after the electrochemical doping process, although there may be a risk of increasing contact resistance for the soaked ATO electrode owing to its nanoparticulate morphology. Figure 4f shows the cycling stability of the unsoaked and soaked ATO electrodes. Clearly, both unsoaked and soaked electrodes have a similar cycling stability, indicating that the soaking treatment will not reduce the cycling stability of ATO nanotubes. The specific capacitance of the soaked ATO electrode decreases slowly with cycle number and still retains more than 78.0% of initial capacitance at the end of 2000 cycles, which is still 2.38 times larger than the initial capacitance of the unsoaked counterpart.

## Conclusions

Soaking ATO nanotube arrays in deionized water at room temperature for a long time can markedly improve their specific surface area. After thermal annealing and potentiodynamically electrochemical doping for the soaked ATO nanotube arrays, they can deliver an areal capacitance of  $20.96 \text{ mF cm}^{-2}$ , nearly three times larger than that of the unsoaked counterparts. The specific capacitance of the soaked ATO electrode decreases slowly with cycle number and still retains more than 78.0% of initial capacitance at the end of 2000 cycles, which is still 2.38 times higher than initial capacitance of the unsoaked one. The technique presented here provides a facile and cost-effective way to change the morphology of ATO nanotubes and increase specific capacitance, making it suitable for industrial applications.

## Acknowledgements

This work was financially supported by the National Natural Science Foundation of China (Grant Nos. 51377085 and 51577093).

## References

- [1] Wu H, Li D, Zhu X, Yang C, Liu D, Chen X, Song Y, Lu L (2014) High-performance and renewable super capacitors based on TiO<sub>2</sub> nanotube array electrodes treated by an electrochemical doping approach. *Electrochim Acta* 116:129–136
- [2] Pan DY, Xi C, Li Z, Wang L, Chen ZW, Luc B, Wu MH (2013) Electrophoretic fabrication of highly robust, efficient, and benign heterojunction photoelectrocatalysts based on graphene-quantum-dot sensitized TiO<sub>2</sub> nanotube arrays. *J Mater Chem A* 1(11):3551–3555
- [3] Li DD, Chang PC, Chien CJ, Lu JG (2010) Applications of tunable tio<sub>2</sub> nanotubes as nanotemplate and photovoltaic device. *Chem Mater* 22(20):5707–5711
- [4] Kim JY, Sekino T, Tanaka SI (2011) Influence of the size-controlled TiO<sub>2</sub> nanotubes fabricated by low-temperature chemical synthesis on the dye-sensitized solar cell properties. *J Mater Sci* 46(6):1749–1757. doi:10.1007/s10853-010-4994-2
- [5] Gui QF, Yu DL, Zhang SY, Xiao HP, Yang CY, Song Y, Zhu XF (2014) Influence of anodizing voltage mode on the nanostructure of TiO<sub>2</sub> nanotubes. *J Solid State Electrochem* 18(1):141–148
- [6] Tian T, Xiao XF, Liu RF, She HD, Hu XF (2007) Study on titania nanotube arrays prepared by titanium anodization in NH<sub>4</sub>F/H<sub>2</sub>SO<sub>4</sub> solution. *J Mater Sci* 42(14):5539–5543. doi:10.1007/s10853-006-1104-6
- [7] Bai J, Zhou BX, Li LH, Liu YB, Zheng Q, Shao JH, Zhu XY, Cai WM, Liao JS, Zou LX (2008) The formation mechanism of titania nanotube arrays in hydrofluoric acid electrolyte. *J Mater Sci* 43(6):1880–1884. doi:10.1007/s10853-007-2418-8
- [8] Lu XH, Wang GM, Zhai T, Yu MH, Gan JY, Tong YX, Li Y (2012) Hydrogenated TiO<sub>2</sub> nanotube arrays for supercapacitors. *Nano Lett* 12(3):1690–1696
- [9] Liu N, Schneider C, Freitag D, Hartmann M, Venkatesan U, Muller J, Spiecker E, Schmuki P (2014) Black TiO<sub>2</sub> nanotubes: cocatalyst-free open-circuit hydrogen generation. *Nano Lett* 14(6):3309–3313
- [10] Anitha VC, Banerjee AN, Dillip GR, Joo SW, Min BK (2016) Nonstoichiometry-induced enhancement of electrochemical capacitance in anodic TiO<sub>2</sub> nanotubes with controlled pore diameter. *J Phys Chem C* 120(18):9569–9580
- [11] Salari M, Konstantinov K, Liu HK (2011) Enhancement of the capacitance in TiO<sub>2</sub> nanotubes through controlled introduction of oxygen vacancies. *J Mater Chem* 21(13):5128–5133
- [12] Richter C, Schmuttenmaer CA (2010) Exciton-like trap states limit electron mobility in TiO<sub>2</sub> nanotubes. *Nat Nanotechnol* 5(11):769–772
- [13] Zhou H, Zhang Y (2013) Enhancing the capacitance of TiO<sub>2</sub> nanotube arrays by a facile cathodic reduction process. *J Power Sources* 239:128–131
- [14] Sun SP, Liao XM, Yin GF, Yao YD, Huang ZB, Pu XM (2016) Enhanced electrochemical performance of TiO<sub>2</sub>

- nanotube array electrodes by controlling the introduction of substoichiometric titanium oxides. *J Alloys Compd* 680:538–543
- [15] Xu J, Wu H, Lu LF, Leung SF, Chen D, Chen XY, Fan ZY, Shen GZ, Li DD (2014) Integrated photo-super capacitor based on bi-polar TiO<sub>2</sub> nanotube arrays with selective one-side plasma-assisted hydrogenation. *Adv Funct Mater* 24(13):1840–1846
- [16] Yu D, Zhu X, Xu Z, Zhong X, Gui Q, Song Y, Zhang S, Chen X, Li D (2014) Facile method to enhance the adhesion of TiO<sub>2</sub> nanotube arrays to Ti substrate. *ACS Appl Mat Interfaces* 6(11):8001–8005
- [17] Li Z, Ding YT, Kang WJ, Li C, Lin D, Wang XY, Chen ZW, Wu MH, Pan DY (2015) Reduction mechanism and capacitive properties of highly electrochemically reduced TiO<sub>2</sub> nanotube arrays. *Electrochim Acta* 161:40–47
- [18] Wu H, Xu C, Xu J, Lu L, Fan Z, Chen X, Song Y, Li D (2013) Enhanced supercapacitance in anodic TiO<sub>2</sub> nanotube films by hydrogen plasma treatment. *Nanotechnology* 24(45):480–487
- [19] Salari M, Aboutalebi SH, Chidembo AT, Nevirkovets IP, Konstantinov K, Liu HK (2012) Enhancement of the electrochemical capacitance of TiO<sub>2</sub> nanotube arrays through controlled phase transformation of anatase to rutile. *Phys Chem Chem Phys* 14(14):4770–4779
- [20] Raj CC, Sundheep R, Prasanth R (2015) Enhancement of electrochemical capacitance by tailoring the geometry of TiO<sub>2</sub> nanotube electrodes. *Electrochim Acta* 176:1214–1220
- [21] Tian J, Zhao ZH, Kumar A, Boughton RI, Liu H (2014) Recent progress in design, synthesis, and applications of one-dimensional TiO<sub>2</sub> nanostructured surface heterostructures: a review. *Chem Soc Rev* 43(20):6920–6937
- [22] Vidyadharan B, Archana PS, Ismail J, Yusoff MM, Jose R (2015) Improved super capacitive charge storage in electrospun niobium doped titania nanowires. *RSC Adv* 5(62):50087–50097
- [23] Krishnan SG, Archana PS, Vidyadharan B, Misnon II, Vijayan BL, Nair VM, Gupta A, Jose R (2016) Modification of capacitive charge storage of TiO<sub>2</sub>, with nickel doping. *J Alloys Compd* 684:328–334
- [24] Patil UM, Kulkarni SB, Jamadade VS, Lokhande CD (2011) Chemically synthesized hydrous RuO<sub>2</sub> thin films for super capacitor application. *J Alloys Compd* 509(5):1677–1682
- [25] Lin YS, Lee KY, Chen KY, Huang YS (2009) Superior capacitive characteristics of RuO<sub>2</sub> nanorods grown on carbon nanotubes. *Appl Surf Sci* 256(4):1042–1045
- [26] Hu CC, Guo HY, Chang KH, Huang CC (2009) Anodic composite deposition of RuO<sub>2</sub> x H<sub>2</sub>O–TiO<sub>2</sub> for electrochemical supercapacitors. *Electrochem Commun* 11(8):1631–1634
- [27] Zhang GG, Huang CJ, Zhou LM, Ye L, Li WF, Huang HT (2011) Enhanced charge storage by the electrocatalytic effect of anodic TiO<sub>2</sub> nanotubes. *Nanoscale* 3(10):4174–4181
- [28] Chen B, Hou JB, Lu K (2013) Formation mechanism of TiO<sub>2</sub> nanotubes and their applications in photoelectrochemical water splitting and supercapacitors. *Langmuir* 29(19):5911–5919
- [29] Guan C, Xia XH, Meng N, Zeng ZY, Cao XH, Soci C, Zhang H, Fan HJ (2012) Hollow core-shell nanostructure super capacitor electrodes: gap matters. *Energy Environ Sci* 5(10):9085–9090
- [30] Wang D, Liu L, Zhang F, Tao K, Pippel E, Domen K (2011) Spontaneous phase and morphology transformations of anodized titania nanotubes induced by water at room temperature. *Nano Lett* 11(11):3649–3655
- [31] Kurian S, Sudhagar P, Lee J, Song D, Cho W, Lee S, Kang YS, Jeon H (2013) Formation of a crystalline nanotube–nanoparticle hybrid by post water-treatment of a thin amorphous TiO<sub>2</sub> layer on a TiO<sub>2</sub> nanotube array as an efficient photoanode in dye-sensitized solar cells. *J Mater Chem A* 1(13):4370–4375
- [32] Song Y, Lv HL, Yang CY, Xiao HP, Chen XY, Zhu XF, Li DD (2014) Enhanced electroactivity at physiological pH for polyaniline in three-dimensional titanium oxide nanotube matrix. *Phys Chem Chem Phys* 16(30):15796–15799
- [33] Chen X, Song Y, Lu L, Cheng C, Liu D, Fang X, Chen X, Zhu X, Li D (2013) Electrochemically hydrogenated TiO<sub>2</sub> nanotubes with improved photoelectrochemical water splitting performance. *Nanoscale Res Lett* 8(1):1–7
- [34] Frackowiak E, Beguin F (2001) Carbon materials for the electrochemical storage of energy in capacitors. *Carbon* 39(6):937–950
- [35] Zhou H, Zhang YR (2014) Electrochemically self-doped TiO<sub>2</sub> nanotube arrays for supercapacitors. *J Phys Chem C* 118(11):5626–5636
- [36] Fabregat-Santiago F, Mora-Sero I, Garcia-Belmonte G, Bisquert J (2003) Cyclic voltammetry studies of nanoporous semiconductors. Capacitive and reactive properties of nanocrystalline TiO<sub>2</sub> electrodes in aqueous electrolyte. *J Phys Chem B* 107(3):758–768
- [37] Li QY, Li ZS, Lin L, Wang XY, Wang YF, Zhang CH, Wang HQ (2010) Facile synthesis of activated carbon/carbon nanotubes compound for super capacitor application. *Chem Eng J* 156(2):500–504
- [38] Liu Y, Wang YZ, Zhang GX, Liu W, Wang DH, Dong YG (2016) Preparation of activated carbon from willow leaves and evaluation in electric double-layer capacitors. *Mater Lett* 176:60–63